

Matter, Volume 2

Supplemental Information

Investigation of Cortisol Dynamics in Human Sweat Using a Graphene-Based Wireless mHealth System

Rebeca M. Torrente-Rodríguez, Jiaobing Tu, Yiran Yang, Jihong Min, Minqiang Wang, Yu Song, You Yu, Changhao Xu, Cui Ye, Waguih William IsHak, and Wei Gao

Matter, Volume 2

Supplemental Information

Investigation of Cortisol Dynamics in Human Sweat Using a Graphene-Based Wireless mHealth System

Rebeca M. Torrente-Rodríguez, Jiaobing Tu, Yiran Yang, Jihong Min, Minqiang Wang, Yu Song, You Yu, Changhao Xu, Cui Ye, Waguih William IsHak, and Wei Gao

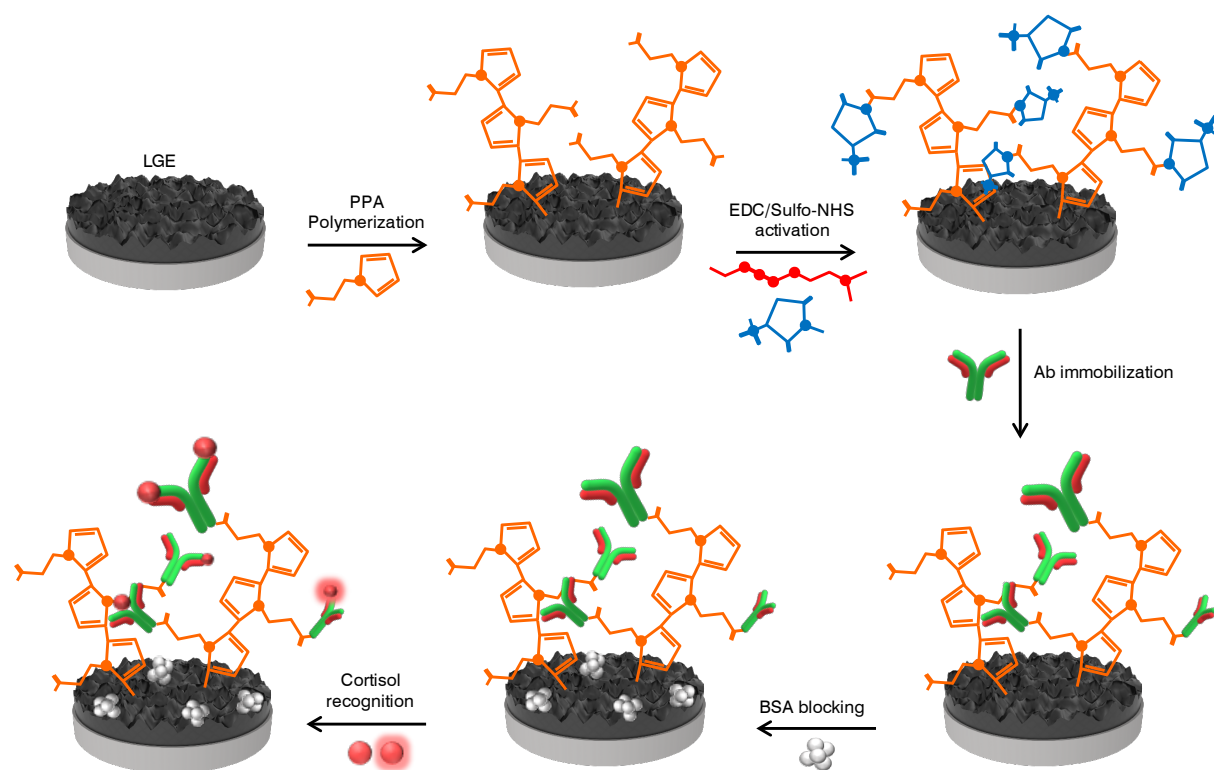


Figure S1. Schematic of modification procedure of the graphene electrode for cortisol sensing.

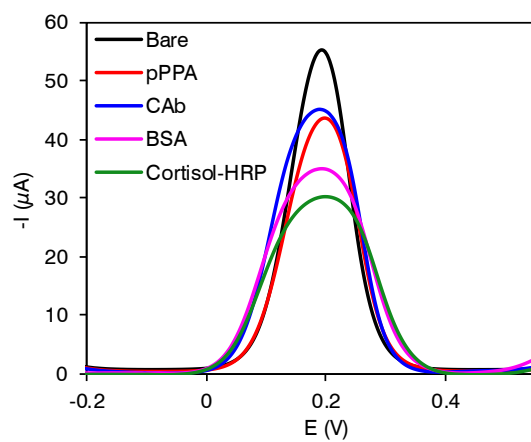


Figure S2. Characterization of the graphene sensor. Differential pulse voltammetry (DPV) in 2.0 mM of $\text{K}_4\text{Fe}(\text{CN})_6/\text{K}_3\text{Fe}(\text{CN})_6$ (1:1) after each modification step.

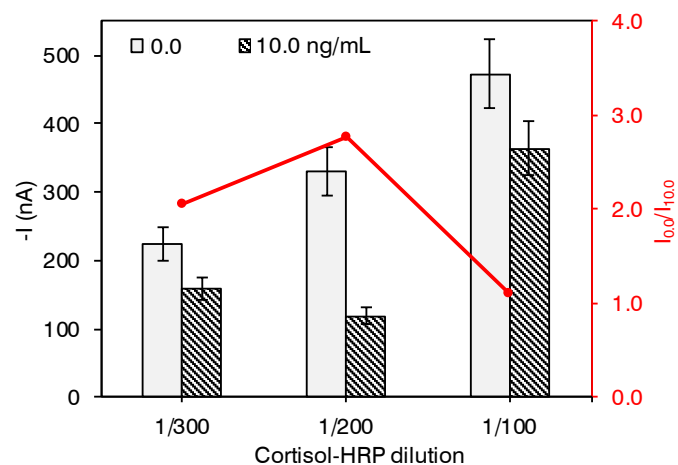


Figure S3. Electrochemical cortisol sensor optimization. Effect of cortisol-HRP dilution factor on amperometric signals. Data are represented as mean \pm SD ($n = 3$).

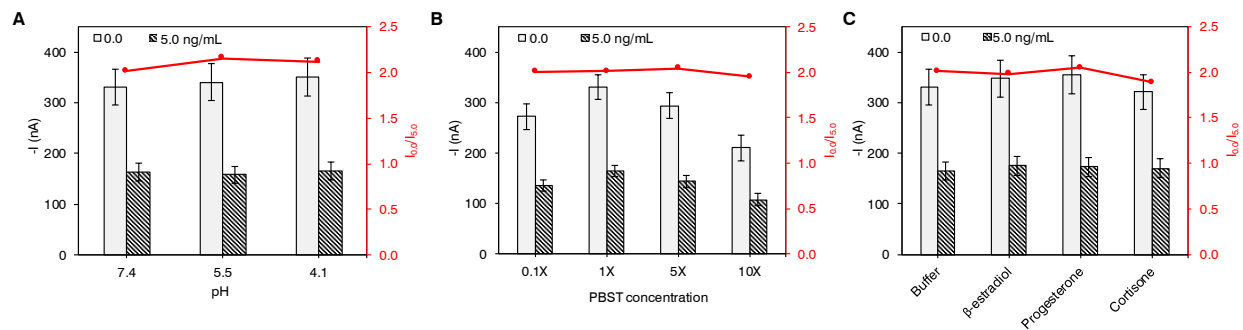


Figure S4. Performance characterization of the graphene-based electrochemical sensors.

Effect of various pHs (A), ionic strengths (B), and presence of interferential molecules (5.0 ng/mL)

(C). PBST, phosphate buffered saline with Tween[®] 20. Data are represented as mean \pm SD ($n = 3$).

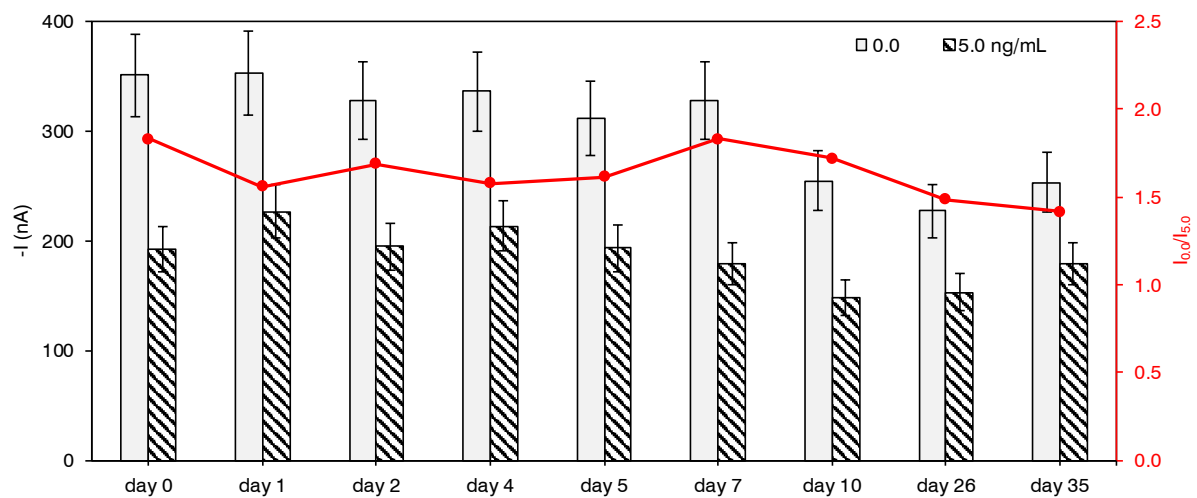


Figure S5. Stability test of the graphene-based electrochemical sensors. Variation of amperometric responses for 0.0 and 5.0 ng/mL cortisol with time. Data are represented as mean \pm SD ($n = 3$).

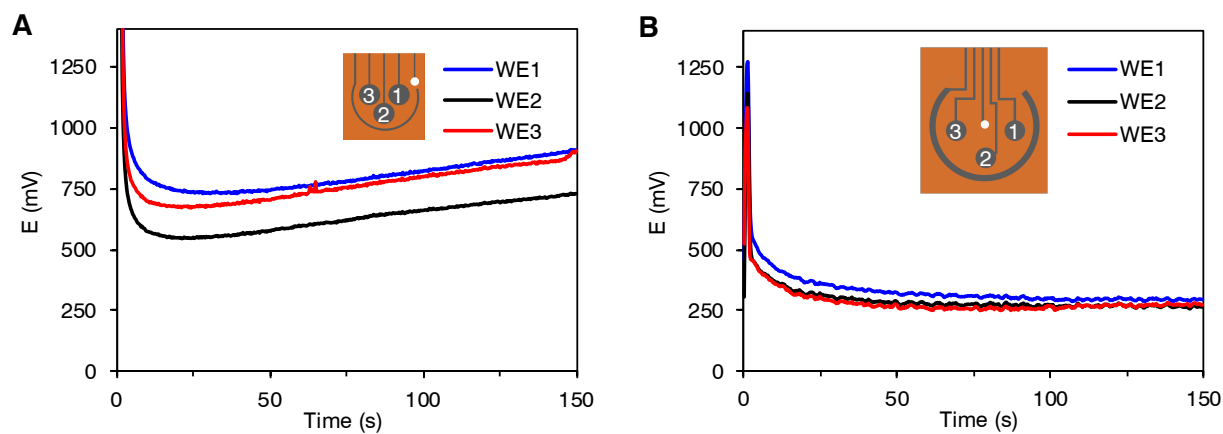


Figure S6. Optimization of platform design. 3-channel amperometric signals obtained with two platform designs in 1,000,000X diluted HRP-cortisol, 2.0 mM HQ and 1.0 mM H_2O_2 in 50 mM phosphate buffer (pH 6.0). The platform with asymmetric working-to-reference design (A) displays larger variations in signals obtained as compared with a symmetric design (B).

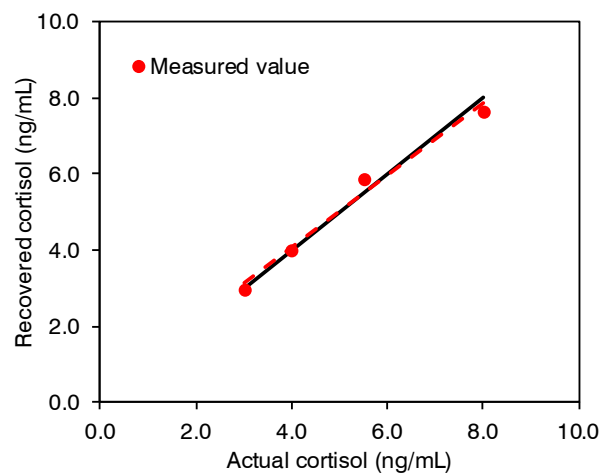


Figure S7. Proportional error evaluated for the GS⁴ based on real sample recovery studies.

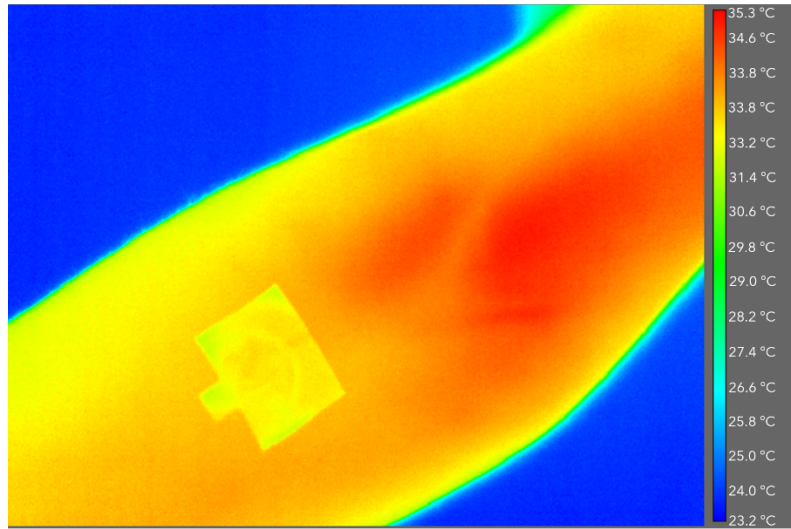


Figure S8. Thermal image of the sensor patch on human forearm.

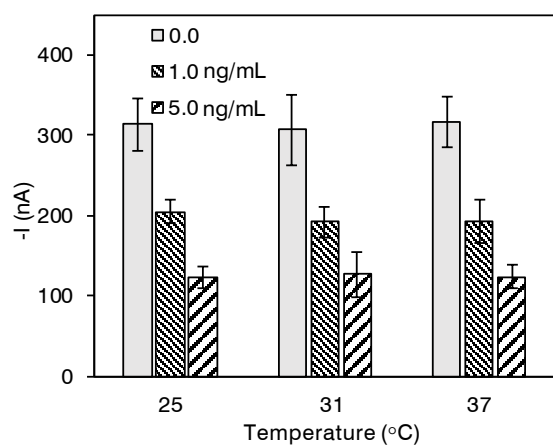


Figure S9. Influence of temperature on sensor performance. Amperometric responses for 0.0, 1.0 and 5.0 ng/mL cortisol incubated at room temperature (25 °C), 31 °C and 37 °C. Data are represented as mean \pm SD ($n = 3$).

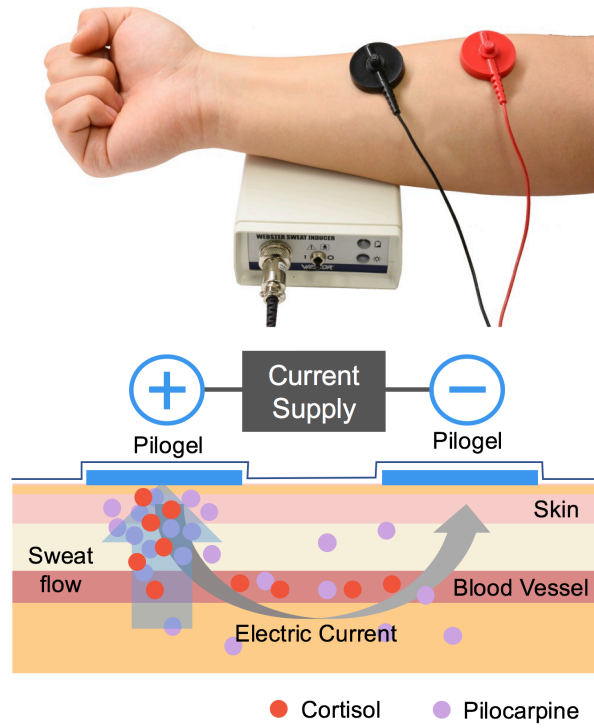


Figure S10. Iontophoresis based sweat sampling. Illustration of iontophoresis-assisted sweat stimulation on a subject's forearm, and principles of sweat stimulation and cortisol excretion in sweat.

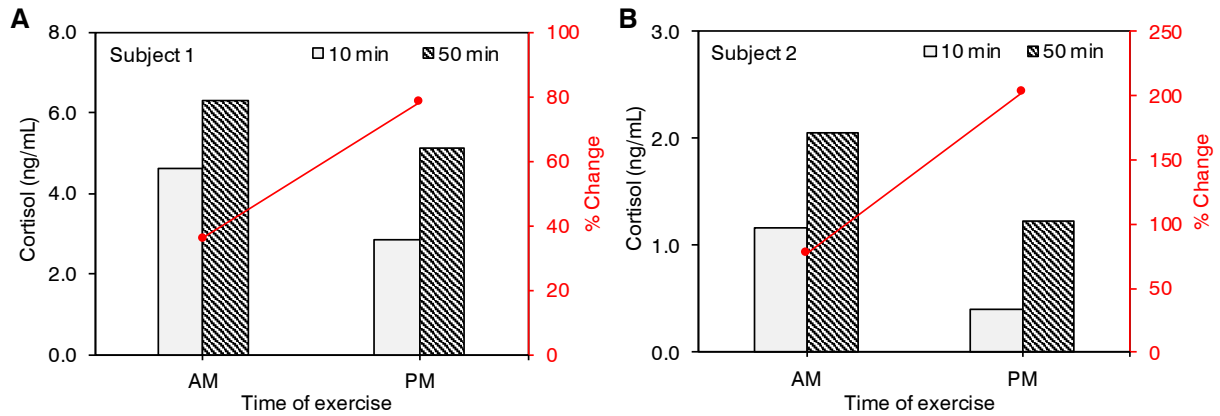


Figure S11. Influence of time of exercise in cortisol variation. Cortisol level evaluated in sweat and its relative percentage change of two healthy subjects before and after physical exercise conducted in the morning (AM) and in the afternoon (PM).

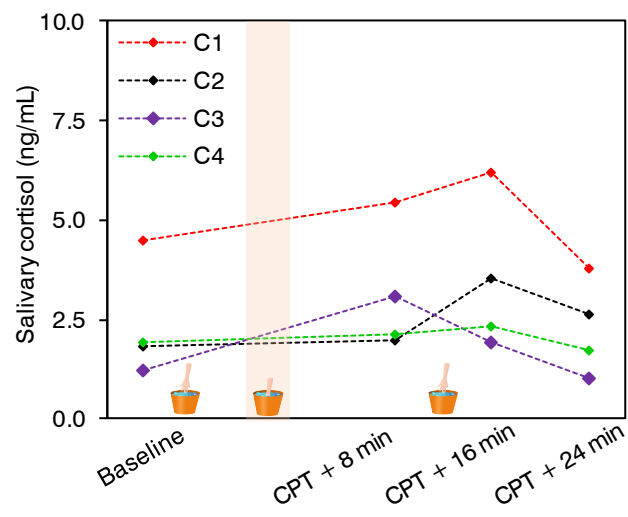


Figure S12. Salivary cortisol at several time points across the cold pressor test for four subjects (C1-C4) from the human study presented in Figure 5.